# Climatology of Lake-Effect Precipitation Events over Lake Champlain

NEIL F. LAIRD AND JARED DESROCHERS

*Department of Geoscience, Hobart and William Smith Colleges, Geneva, New York*

MELISSA PAYER

*Chemical, Earth, Atmospheric, and Physical Sciences Department, Plymouth State University, Plymouth, New Hampshire*

(Manuscript received 29 November 2007, in final form 11 June 2008)

ABSTRACT

This study provides the first long-term climatological analysis of lake-effect precipitation events that developed in relation to a small lake (having a surface area of $\leq$1500 km$^2$). The frequency and environmental conditions favorable for Lake Champlain lake-effect precipitation were examined for the nine winters (October–March) from 1997/98 through 2005/06. Weather Surveillance Radar-1988 Doppler (WSR-88D) data from Burlington, Vermont, were used to identify 67 lake-effect events. Events occurred as 1) well-defined, isolated lake-effect bands over and downwind of the lake, independent of larger-scale precipitating systems (LC events), 2) quasi-stationary lake-effect bands over the lake embedded within extensive regional precipitation from a synoptic weather system (SYNOP events), or 3) a transition from SYNOP and LC lake-effect precipitation. The LC events were found to occur under either a northerly or a southerly wind regime. An examination of the characteristics of these lake-effect events provides several unique findings that are useful for comparison with known lake-effect environments for larger lakes. January was the most active month with an average of nearly four lake-effect events per winter, and approximately one of every four LC events occurred with southerly winds. Event initiation and dissipation occurred on a diurnal time scale with an average duration of 12.1 h. In general, Lake Champlain lake-effect events 1) typically yielded snowfall, with surface air temperatures rarely above 0°C, 2) frequently had an overlake mesolow present with a sea level pressure departure of 3–5 hPa, 3) occurred in a very stable environment with a surface inversion frequently present outside the Lake Champlain Valley, and 4) averaged a surface lake–air temperature difference of 14.4°C and a lake–850-hPa temperature difference of 18.2°C. Lake Champlain lake-effect events occur within a limited range of wind and temperature conditions, thus providing events that are more sensitive to small changes in environmental conditions than are large-lake lake-effect events and offering a more responsive system for subsequent investigation of connections between mesoscale processes and climate variability.

## 1. Introduction

The development of lake-effect snowstorms and their characteristics (e.g., snowfall) have long been documented for the Great Lakes region (e.g., Dole 1928; Remick 1942; Peace and Sykes 1966; Dewey 1975; Braham and Dungey 1984; Niziol et al. 1995; Laird et al. 2001; Rodriguez et al. 2007). Investigations of lake-effect snowstorms in association with smaller lakes have been much fewer in number and were conducted mostly within the last decade. These studies have discussed lake-effect snow over the Great Salt Lake (Carpenter 1993; Steenburgh et al. 2000; Steenburgh and Onton 2001; Onton and Steenburgh 2001), New York State (NYS) Finger Lakes (Cosgrove et al. 1996; Watson et al. 1998; Sobash et al. 2005), Lake Champlain (Tardy 2000; Payer et al. 2007), and small lakes in the western and midwestern United States (Wilken 1997; Cairns et al. 2001; Schultz et al. 2004). Several of these storms have produced significant impacts despite their localized spatial extent. For example, Cairns et al. (2001) examined a lake-effect snow event associated with Lake

*Corresponding author address:* Neil F. Laird, Dept. of Geoscience, Hobart and William Smith Colleges, 4002 Scandling Center, Geneva, NY 14456.
E-mail: laird@hws.edu

DOI: 10.1175/2008JAMC1923.1

Tahoe that produced over 53 cm (23 in.) in Carson City, Nevada, during a 2-day period. Steenburgh and Onton (2001) conducted a multiscale analysis of an early December lake-effect snowstorm that developed over the Great Salt Lake and resulted in 36 cm (14 in.) of snow near Salt Lake City, Utah. during a 15-h time period. In addition, Tardy (2000) reported that Lake Champlain lake-effect storms can generate localized snowfall totals comparable to synoptic winter storms and on occasion have produced snow squalls with visibilities of less than 400 m (0.25 mi.) and up to 33 cm (13 in.) of snow in a 12-h period.

Several climatological studies have investigated the frequency and associated conditions of lake-effect storms for the Great Lakes. These studies have focused on the temporal and spatial variations of lake-effect snowfall (Jiusto and Kaplan 1972; Braham and Dungey 1984; Kelly 1986; Norton and Bolsenga 1993; Kunkel et al. 2002; Burnett et al. 2003; Kristovich and Spinar 2005); the frequency, conditions, and mesoscale structure of single or multiple lake events (Forbes and Merritt 1984; Kristovich and Steve 1995; Weiss and Sousounis 1999; Rodriguez et al. 2007); and the occurrence of thundersnow (Schultz 1999). Few studies have conducted lake-effect climatological analyses for lakes smaller than the Great Lakes. Carpenter (1993) and Steenburgh et al. (2000) studied the frequency and characteristics of lake-effect snowstorms of the Great Salt Lake. Sobash et al. (2005) and Laird et al. (2009) conducted a more recent climatological study of lake-effect precipitation events associated with the NYS Finger Lakes. In addition, a climatological study of Lake Tahoe lake-effect events is under way (S. J. Underwood, Nevada State Climatologist, 2007, personal communication).

The current investigation was undertaken to determine the frequency and environmental conditions favorable for the development of lake-effect precipitation in the vicinity of Lake Champlain by examining the nine winters (October–March) from 1997/98 through 2005/06. Lake Champlain is a north–south-oriented lake located along the border of northern New York and Vermont with the Adirondack Mountains to the west and the Green Mountains to the east (Fig. 1). Lake Champlain is approximately 193 km long and has a maximum width of 19 km, and the surface area of the lake (1127 $km^2$) is considerably smaller than that of Lake Ontario (18 960 $km^2$), the smallest of the Great Lakes, and the Great Salt Lake (4400 $km^2$). The lake has an average depth of 20 m and maximum depth of 122 m, with an average lake level between 29 and 30 m above mean sea level (Tardy 2000).

The data and methods used in the study, including the criteria for identifying several types of Lake Champlain lake-effect precipitation, are described in section 2. Section 3 presents the frequency, synoptic-scale environments, and mesoscale conditions. A discussion of the Lake Champlain lake-effect results is presented in section 4.


FIG. 1. Topographic map of Lake Champlain Valley showing locations of observing sites. Inset map shows larger region with Lake Champlain highlighted.

## 2. Data and methods

The climatological study incorporates a variety of datasets (i.e., surface, radar, sounding, lake temperature, and regional reanalysis) to compose a coherent understanding of the characteristics of Lake Champlain lake-effect storms and the mesoscale and synoptic environments favorable for storm development. There are several unique aspects of this study afforded by the locations of the observing sites (Fig. 1). The National

Weather Service (NWS) Weather Surveillance Radar-1988 Doppler (WSR-88D) positioned in Burlington, Vermont, along the eastern shore of Lake Champlain provides an exceptional view of the full extent of lake-effect precipitation bands that developed during events. Payer et al. (2007) and Tardy (2000) have previously demonstrated the utility of the Burlington WSR-88D radar to observe Lake Champlain lake-effect snowbands. In addition, the four surface stations used for climatological analyses allowed for a comparison of conditions to the north of the Lake Champlain Valley, along the eastern and western shorelines of Lake Champlain, and at an overlake location. Also unique and important to this study are the measurements of (a) Lake Champlain water temperatures at a site in close proximity to the surface station along the eastern shore and (b) atmospheric temperature profiles at Burlington International Airport (KBTV) from aircraft equipped with the Aircraft Communication Addressing and Reporting System (ACARS).

### *a. Radar data*

Burlington WSR-88D radar (KCXX) data were used to identify lake-effect precipitation events for the nine winters (October–March) from 1997/98 through 2005/06. The review of the nine winters was primarily conducted using KCXX level-II data obtained through the National Climatic Data Center (NCDC) Hierarchical Data Storage System. Level-III image products were examined, when available, for time periods for which level-II data were not archived. During the process of identifying Lake Champlain lake-effect events, over 233 000 radar volumes (i.e., reflectivity and radial velocity data for multiple elevation scans) were displayed and inspected with the GRLevel2 and GRLevel3 programs produced by Gibson Ridge Software, LLC. Fewer than 3% (48) of the total 1645 days composing the nine-winter period had radar data unavailable for a time period longer than the average duration of a Lake Champlain lake-effect event (12.1 h). These extended time periods of missing data were considered in the determination of the monthly and annual frequencies.

Inspection of the radar data yielded the identification of 67 lake-effect precipitation events. Several indicators were used to establish a justified and repeatable method for identification of lake-effect precipitation based solely on the radar data. This method was intended to limit possible predisposition regarding favorable mesoscale and synoptic conditions necessary for Lake Champlain lake-effect precipitation. The indicators were developed based on multiple passes through the radar data for the nine-winter period and knowledge gained from previous studies of lake-effect precipitation that incorporated considerable radar analyses for small lakes (e.g., Steenburgh et al. 2000; Tardy 2000) and large lakes (e.g., Kelly 1986; Kristovich et al. 1999; Grim et al. 2004). The use of computer animation of the radar reflectivity field for multiple radar beam elevation angles was found to be important to developing and implementing the method for identification of lake-effect events. Three indicators specific to this investigation were the following:

1) *The existence of coherent precipitation in the reflectivity field that developed over Lake Champlain and remained quasi stationary with a distinct spatial connection to the lake* (e.g., substantial portion of precipitation over the lake and confined to lowlands in the Lake Champlain Valley with topographic elevations of <150 m above lake level). The temporally and spatially consistent nature of the mesoscale precipitation field in the vicinity of Lake Champlain, as demonstrated in animations of the radar reflectivity field, was the most important aspect of this indicator. The radar reflectivity on 15 December 2004 provides an example of lake-effect precipitation having both overlake and quasi-stationary features (Figs. 2a–c).
2) *The precipitation was composed of mesoscale structural features that were clearly distinguishable from extensive or transitory regions of precipitation and were generally below a height of 2 km*. The precipitation typically consisted of mesoscale bands with an orientation at a small angle relative to the major axis of the lake; however, the band orientation was not a limiting factor when considering a designation as lake-effect precipitation. The radar reflectivity on 27 November 2002 provides an example of lake-effect precipitation occurring during a time period with variable widespread synoptic precipitation also in the region (Figs. 2d–f).
3) *The precipitation often demonstrated increasing reflectivity, depth, or spatial coverage at locations along the downwind extent of the mesoscale band with some portion of the mesoscale precipitation remaining over the lake* (Fig. 2). Events were not designated as lake-effect precipitation when the mesoscale precipitation developed away from the shoreline of Lake Champlain (>10 km) and was not present over the lake. These were suspected to be topographically forced precipitation events rather than thermally driven lake-effect events.

The timing of initiation and dissipation of each lake-effect event was determined, as well as the overlake and inland regions impacted by precipitation. Information

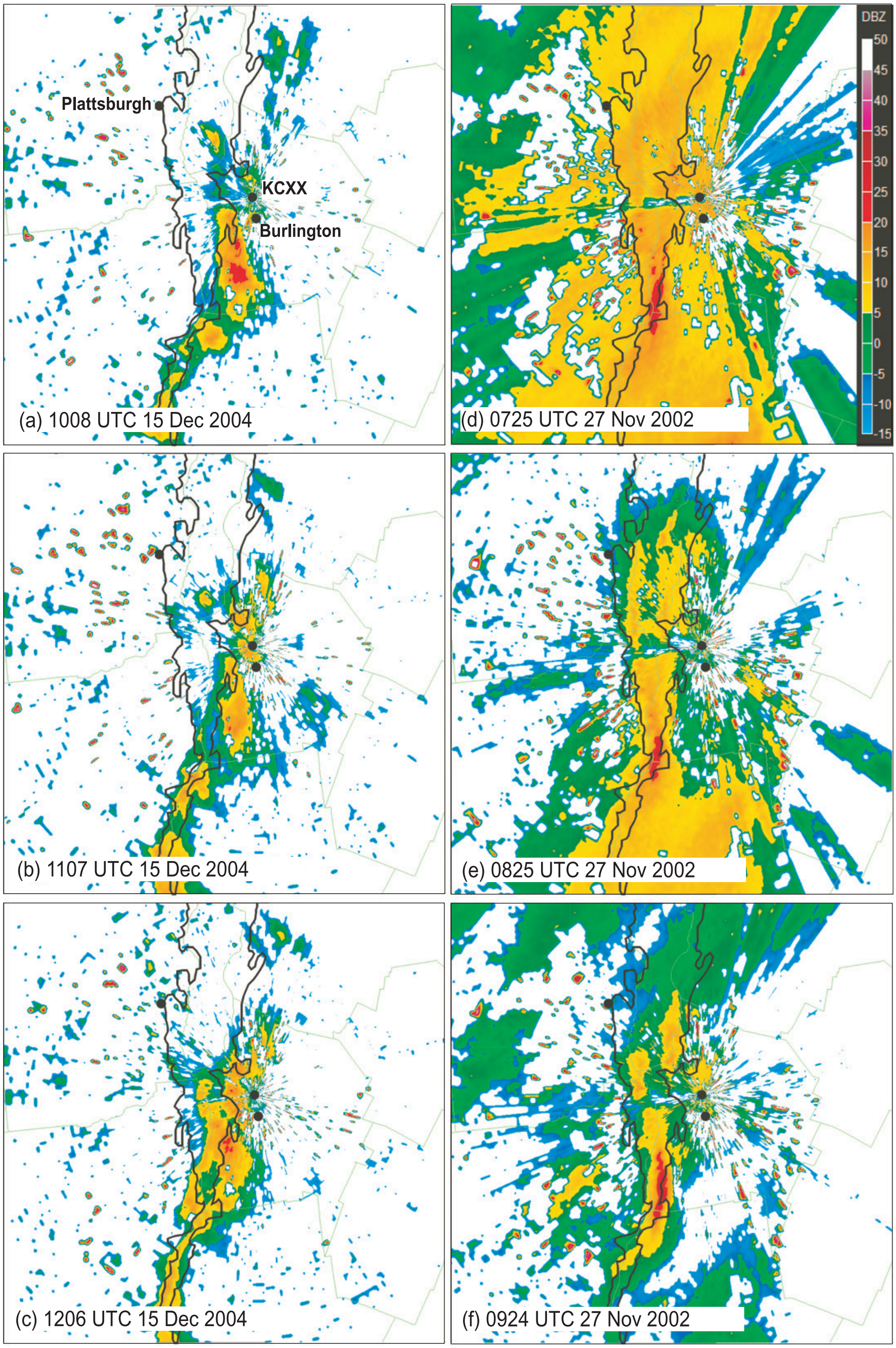


FIG. 2. Time series of Burlington WSR-88D (KCXX) radar reflectivity fields at 0.5° elevation on (a)–(c) 15 Dec 2004 and (d)–(f) 27 Nov 2002 that demonstrate the first and second indicators, respectively, used in the method for identifying Lake Champlain lake-effect precipitation events.

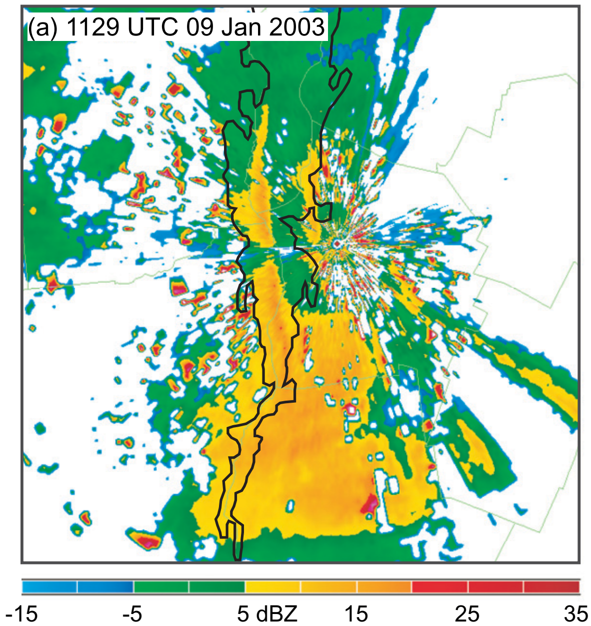


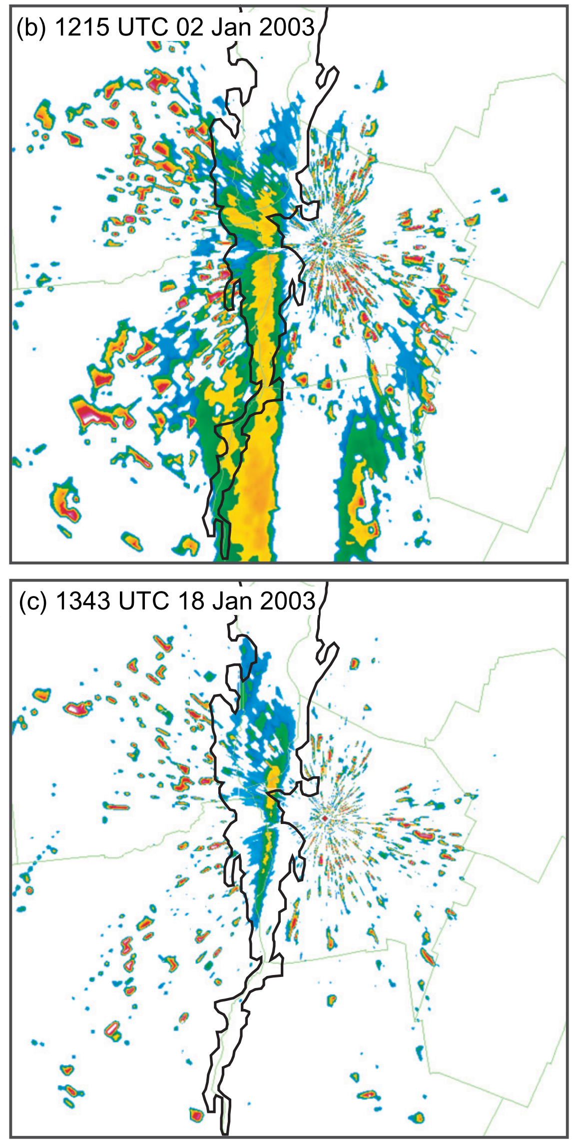


FIG. 3. Examples of KCXX radar reflectivity fields at 0.5° elevation for (a) lake-effect precipitation embedded within a precipitation shield associated with a synoptic weather system (SYNOP), (b) lake-effect precipitation during northerly winds (LC-North), and (c) lake-effect precipitation during southerly winds (LC-South).

about the amount of precipitation produced during these events was not available because of the localized nature of the precipitation and the very limited distribution of NWS and cooperative observer surface measurement sites within the Lake Champlain Valley.

Events that were identified during the nine winters often had similar structural characteristics in the evolution of the lake-effect precipitation. Lake Champlain lake-effect events were found to occur as 1) well-defined, isolated precipitation bands over and downwind of the lake, independent of larger-scale precipitating systems (hereinafter referred to as LC events), 2) quasi-stationary mesoscale precipitation bands over the lake embedded within extensive regional precipitation from a synoptic weather system (SYNOP events), or 3) a transition between SYNOP and LC lake-effect precipitation. An unexpected fact is that lake-effect precipitation bands during LC events occurred with either north (LC-North) or south (LC-South) prevailing surface winds. The KCXX radar reflectivity field showing events of the three distinct lake-effect types (SYNOP, LC-North, and LC-South) is provided in Fig. 3. A case study presented by Payer et al. (2007) provides additional analyses and discussion of the 18 January 2003 LC-South lake-effect snow event (Fig. 3c).

### b. *Hourly surface data*

Data from four surface stations permitted a comparison of meteorological conditions among sites outside the Lake Champlain Valley, at two nearshore locations, and at an overlake location (Fig. 1). The St. Hubert Airport station in Quebec, Canada, (CYHU) is positioned about 60 km north of Lake Champlain and provided information concerning the airmass characteristics outside of the Lake Champlain Valley. KBTV, located on the eastern shore in Burlington, and Clinton County Airport (KPLB), located farther north on the western shore in Plattsburgh, New York, provided meteorological conditions in the nearshore regions (<4 km) of Lake Champlain. The Vermont Monitoring Cooperative Colchester Reef (VMCR) meteorological station, which has operated on the navigational light tower at Colchester Reef since July of 1996, provided hourly surface measurements over central Lake Champlain.

The event-average wind direction from KBTV was used to differentiate LC-North and LC-South lake-effect events. Wind directions reported at KBTV were found to be more consistent with the overlake KCXX radial velocity field in comparison with KPLB measurements and were available for the entire nine-winter time period. An average northerly wind direction at KBTV between 271° and 89° designated an LC-North event. The occurrence of an average southerly wind direction between 91° and 269° corresponded to LC-South events. During the nine-winter period, 5 of the 48 LC events had either calm or weak variable winds ($<2$ m s$^{-1}$) and were not classified as LC-North or LC-South. These events, referred to as LC-Calm, likely occurred with a primary contribution from land breezes resulting in weak easterly flow at KBTV. In a few LC-Calm cases, conditions made a transition between weak northerly and southerly wind regimes while the LC band remained coherent and experienced nearly a 180° shift in orientation along the major lake axis (e.g., 23 January 1998).

Surface data for stations KBTV, KPLB, and CYHU were obtained from the NCDC online archive using the Global Hourly Surface Data product. The number of hourly observations collected during SYNOP, LC-North, LC-South, and LC-Calm events total 132, 527, 84, and 48, respectively. The listed number of hourly observations takes into account time periods of lake-effect precipitation that occurred during SYNOP and LC portions of transitional events. Data from KPLB were unavailable for the first two winters of the study (1997/98 and 1998/99). The VMCR station data were obtained from the Vermont Monitoring Cooperative through their online historical data archive (http://sal.snr.uvm.edu/vmc/air/). Standard surface meteorological parameters, such as temperature, dewpoint temperature, wind direction and speed, and sea level pressure, were available for all stations.

### c. Lake temperature and ice cover data

Archived daily water temperature data collected at the King Street Ferry dock (KSFD) in Burlington were obtained from the NWS Forecast Office. Lake temperature measurements were acquired at a depth of approximately 2 m and have been recorded beginning in 1972, with data for January, February, and March only available since 1986. Manley et al. (1999) showed that Lake Champlain has a nearly isothermal vertical temperature profile from mid-November to mid-May as a result of cooling and wind-forced mixing. This suggests that the KSFD water temperature measurements at a 2-m depth are likely representative of Lake Champlain surface water temperatures during wintertime (October–March) periods when this region of Lake Champlain is free of ice cover.

Consistent ice cover data for Lake Champlain during the period of study were difficult to obtain. This information was acquired from two different sources and consisted of ice cover freeze and thaw dates for the central basin of Lake Champlain, the widest portion of the lake offshore Burlington. Ice information was obtained from the National Snow and Ice Data Center using the Global Lake and River Ice Phenology database (Benson and Magnuson 2006) for the winters of 1997–2001 (http://nsidc.org/data/lake_river_ice/). Additional information on freeze date for the winters of 2003–05 was available from the Lake Champlain Basin Program (http://www.lcbp.org/).

### d. Sounding data

Soundings from Albany, New York, (ALB) and Maniwaki, Quebec, Canada, (WMW) were obtained from the Plymouth State University online archives (http://vortex.plymouth.edu). A total of 145 soundings (73 forALB and 72 for WMW) that occurred during event time periods provided information for 52 of the 67 events. The remaining 15 events occurred outside the hours for which standard operational soundings were available (0000 and 1200 UTC). The ALB and WMW stations are both located >150 km from Lake Champlain (Fig. 1 inset) and are used to examine the regional atmospheric structure and stability. ACARS data were also available from commercial aircraft descents and ascents at KBTV. An additional 24 ACARS soundings were available for events during the winters of 2002–05 and were obtained from the online retrieval system maintained by the Global Systems Division of the National Oceanic and Atmospheric Administration Earth System Research Laboratory (NOAA/ESRL; http://amdar.noaa.gov/). A comparison of the sounding information from ALB, WMW, and ACARS is provided in section 3d.

## 3. Results

Sixty-seven lake-effect events were identified using KCXX radar data for the nine winters studied. The lake-effect event types consisted of 32 LC-North, 11 LC-South, 5 LC-Calm, 10 SYNOP, and 9 transitional cases containing time periods of LC and SYNOP lake-effect precipitation. Information on all 67 events is provided in section 3a and the appendix. The environmental conditions that occurred during LC-North, LC-South, and SYNOP lake-effect precipitation (including during transitional cases) are the focus of the presentation in sections 3b–d.

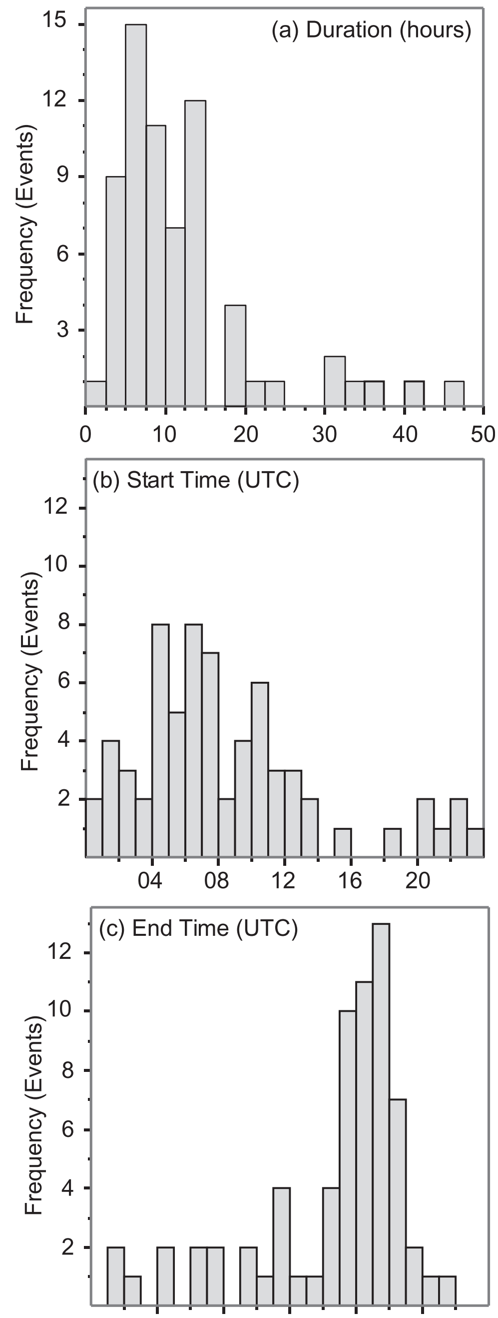


FIG. 4. Histograms showing the event distribution of (a) duration, (b) start time, and (c) end time.

### *a. Event duration, timing, and frequency*

The average duration of Lake Champlain lake-effect events was found to be 12.1 h—significantly shorter than intense Great Lakes lake-effect events, which commonly last multiple days. These events are also shorter than Great Salt Lake lake-effect events identified by Steenburgh et al. (2000), which typically had durations >13 h. A large percentage of Lake Champlain events (55 events or 82.1%) had durations <15 h, and only seven events continued for more than 24 h (Fig. 4a). Transitional events had the longest duration on average (16.6 h) because most of these cases began with a lake-effect band embedded within widespread precipitation (SYNOP) and shifted to an isolated LC-North snowband during the latter stage of the event. LC-south lake-effect precipitation was not observed during transitional events. On average, LC-North events had longer durations than LC-South events, with average durations of 13.6 and 9.3 h, respectively.

The timing of Lake Champlain lake-effect events appears to be strongly linked to diurnal atmospheric variations. Event initiation typically occurred during the overnight and early-morning time period (0400–1100 UTC, or 2300–0600 LST). Although minimum air temperatures and maximum lake–air temperature differences associated with diurnal variations will usually occur just prior to sunrise (1130–1230 UTC for Burlington from October to March), the broadening of the frequency maximum in start times (Fig. 4b) is likely associated with variations in frontal passage times. Regardless of the hour, a wintertime cold-frontal passage can provide the primary forcing conditions for lake-effect events: the introduction of a polar air mass into the Lake Champlain Valley region.

A more distinct maximum between 1500 and 1800 UTC (1000–1300 LST) was present for the timing of event dissipation (Fig. 4c). Nearly 60% of all lake-effect events dissipated during this 4-h time period. The KCXX radar reflectivity field often showed either progressively weakening reflectivity associated with the lake-effect band or that the coherent lake-effect band would segment into cellular convective elements and dissipate.

The distribution of lake-effect event start and end times for Lake Champlain is consistent with results found for the Great Salt Lake by Steenburgh et al.

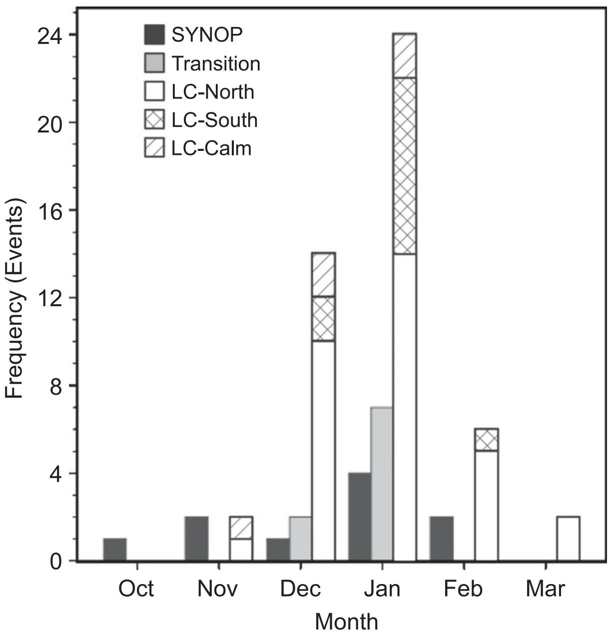


FIG. 5. Seasonal distribution of number of events for each Lake Champlain lake-effect type.

(2000) and the diurnal variations in lake-effect snowfall for Lakes Superior and Michigan (Kristovich and Spinar 2005). Steenburgh et al. (2000) found that 13 of their 16 well-defined events began during the 0000–1200 UTC time period. Using hourly snowfall measurements, Kristovich and Spinar (2005) found a distinct morning maximum and afternoon/evening minimum in lake-effect precipitation frequency during a five-winter time period.

There was a substantial amount of interannual and intraseasonal variability in the frequency of Lake Champlain lake-effect events during the nine winters studied (Fig. 5). The appendix provides a table that contains information for each event identified in this investigation. The least active winter (2001/02) had only 2 events, whereas 11 events were recorded during each of the most active winters (2002/03 and 2004/05). January was the most active month, with an average of nearly 4 events per winter (i.e., 35 events during nine winters). December and February had considerably fewer total events, with 17 and 8, respectively. LC events represented a large percentage of all events during December, January, and February, with 82%, 69%, and 75%, respectively. Nearly one of every four LC events on average had winds from the south (i.e., LC-South), with a larger percent (33%) occurring during January.

The notable decrease in events during February may be linked to a reduction of open water resulting from significant ice cover on Lake Champlain—in particular, in the shallow southern-bay and northern-island regions. The average ice-closing date for Lake Champlain is 8 February based on ice cover information from the Global Lake and River Ice Phenology data for the winters of 1816–2001 (Benson and Magnuson 2006). Available ice cover records show that Lake Champlain completely closed for four winters during the study period and had an average ice-closing date of 19 February. Although several winters did not experience a closing of Lake Champlain by ice cover, the ice conditions may have resulted in a significant decrease in open-water area (i.e., overlake fetch) and a reduction in the surface sensible and latent heat fluxes (Gerbush et al. 2008), which would influence the ability to support lake-effect snowstorm development (Cordeira and Laird 2008).

### b. Synoptic patterns

The sea level pressure (SLP) and surface temperature distributions for SYNOP, LC-North, and LC-South lake-effect precipitation events are shown in Fig. 6. These analyses represent composites from all the 6-h National Centers for Environmental Prediction–National Center for Atmospheric Research reanalysis data (Kalnay et al. 1996) available during times of Lake Champlain lake-effect precipitation. The SYNOP, LC-North, and LC-South composite analyses were produced using NOAA/ESRL Physical Science Division online utilities (http://www.cdc.noaa.gov/Composites/Hour/) and are composed of 18, 91, and 13 time periods, respectively.

The SYNOP composite analyses (Figs. 6a,b) show 1) the presence of low pressure off the New England coast and an area of high pressure over the western Great Lakes, 2) a relatively large pressure gradient in the vicinity of the Lake Champlain Valley, suggesting strong northerly surface winds, and 3) below-freezing temperatures (from −9° to −13°C) over the Lake Champlain region. The LC-North composite analyses (Figs. 6c,d) show 1) an eastward progression of the SLP pattern with high pressure centered over southern Ontario, Canada, and a southward-oriented trough positioned east of the Canadian maritime provinces, 2) a small pressure gradient over northern New York and Vermont leading to weak northerly winds, and 3) a southward advancement of the polar air mass into the northeastern United States, with temperatures in the range from −16° to −20°C over the Lake Champlain region. The LC-South composite analyses (Figs. 6e,f) show 1) a significant shift in the SLP pattern, with low pressure centered over the western Great Lakes and a ridge axis along the Appalachian Mountains extending northward from a high pressure center in the southeast United States, 2) a small pressure gradient associated

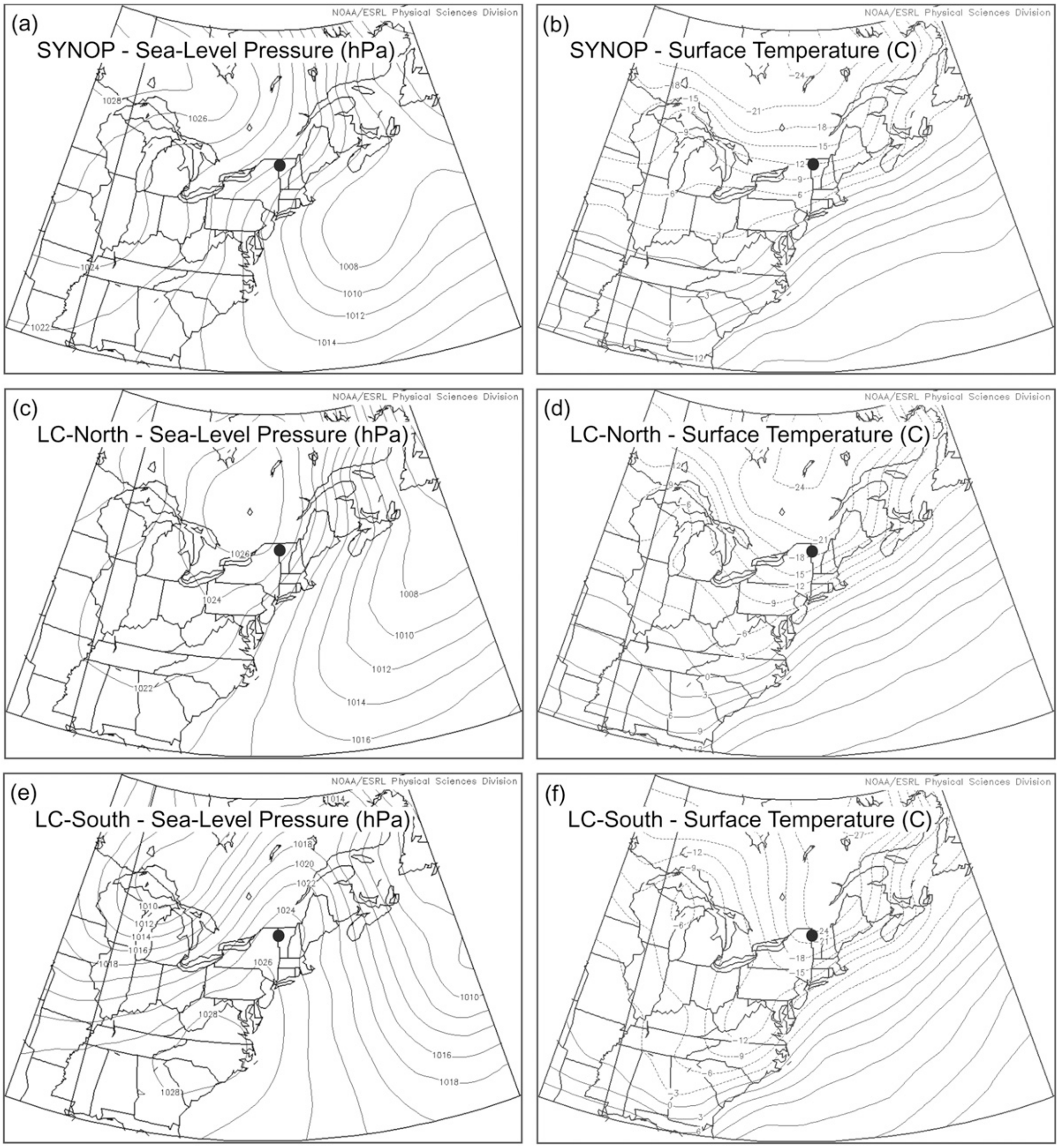


FIG. 6. Composite (left) SLP and (right) surface temperature maps for (a), (b) SYNOP, (c), (d) LC-North, and (e), (f) LC-South event types. Isobars and isotherms are plotted using a 4-hPa and 3°C contour interval, respectively, with negative temperatures denoted using dashed contours. The black circle shows the location of Lake Champlain. The composite maps were generated using the NOAA/ESRL Physical Sciences Division Web site (http://www.cdc.noaa.gov/).

with the ridge axis positioned over Lake Champlain, and 3) a region of below-freezing temperatures extending farther southward (especially along the Appalachian Mountains), with temperatures ranging from −20° to −24°C over the Lake Champlain region. These composite analyses provide a large-scale framework that complements the surface and sounding data presented in sections 3c and 3d.

### c. *Hourly surface observations*

The surface meteorological conditions that occurred during LC-North, LC-South, and SYNOP lake-effect precipitation (including transitional cases) are the focus of the analyses presented in this section. The hourly observations from stations KBTV, KPLB, CYHU, and VMCR are presented using comparative box plots

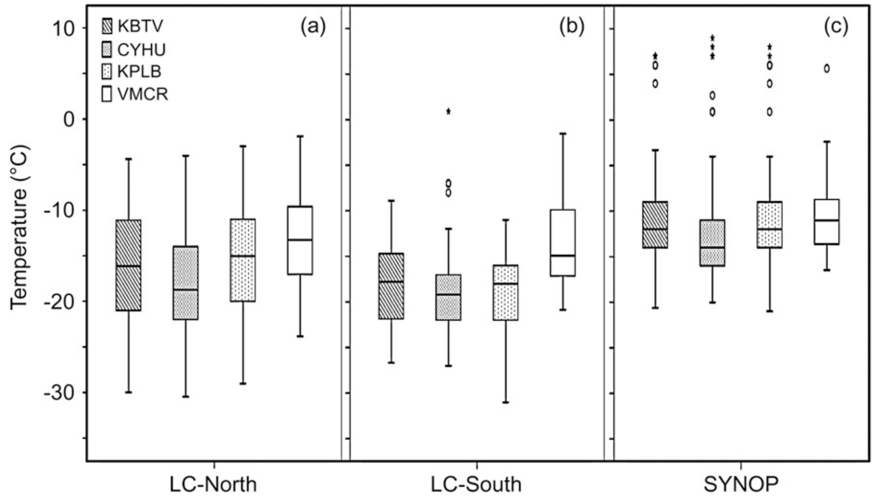


FIG. 7. Box plots showing distributions of temperature (°C) at four surface sites (KBTV, CYHU, KPLB, and VMCR) for (a) LC-North, (b) LC-South, and (c) SYNOP events. Asterisks represent extreme values, and open circles represent outliers (see text for description of outliers and extreme values).

produced with SPSS, Inc., proprietary statistical software. The box of the plot encloses the middle half of the sample, with an end at the upper and lower quartiles. Thus, the box represents the interquartile range of the data sample. The line across the central portion of the box designates the sample median. Values that are greater than 3 times the interquartile range outside the box are denoted by asterisks and are identified as extreme values. Values that are between 1.5 and 3.0 times the interquartile range outside the box are identified with open circles and represent outliers. In SPSS, extremes and outliers are designated relative to a statistically normal distribution. The box plot whiskers represent the minimum and maximum values not marked as extreme or outlier data points. Several variables are examined and discussed: temperature, lake–air temperature difference $\Delta T$, dewpoint temperature, wind speed and direction, and sea level pressure. Statistical comparative analyses were conducted with a two-independent-samples nonparametric test (the Mann–Whitney $U$ test), which does not assume data are normally distributed or have equal variance, and a critical $Z$ value of 1.96 (significance level $p \leq 0.05$) was used to measure significant differences.

### 1) TEMPERATURES

Surface temperatures at all stations were very rarely above freezing (Fig. 7), which suggests that most Lake Champlain precipitation bands resulted in lake-effect snowfall. In contrast, Great Lakes lake-effect cloud and precipitation climatological studies have shown that near-lake surface temperatures can commonly be above freezing, resulting in lake-effect rain (e.g., Miner and Fritsch 1997). For the nine winters studied for Lake Champlain, only during the single early season (i.e., October) SYNOP event were temperatures >0°C (i.e., 6°–9°C), suggesting precipitation fell as lake-effect rain.

Notable temperature variations were found among LC-North, LC-South, and SYNOP lake-effect event types (Fig. 7). SYNOP events were the warmest, with a relatively small spread in temperatures and the interquartile range occurring between −9° and −16°C, regardless of station. LC-North events were colder on average than SYNOP events and show a slightly larger variation in temperature range. Of interest is that LC-South events tended to have the coldest temperatures. The four-station group means for SYNOP, LC-North, and LC-South are −11.2°, −16.1°, and −19.5°C, respectively. Statistical analysis established that temperatures for LC-North, LC-South, and SYNOP all differed significantly.

The variation in temperature seen across lake-effect event types is consistent with the differences in large-scale setting presented in Fig. 6. The warmest temperatures during SYNOP events result from Lake Champlain being in close proximity to the eastward-exiting low pressure (Fig. 6a) and the occurrence of SYNOP events at the early stages of the southward intrusion of the polar air mass (Fig. 6b). LC-North events occur as high pressure to the west of Lake Champlain progresses eastward (Fig. 6c) and the polar air mass becomes more established across the northeastern United States (Fig. 6d). LC-South events take place near the latter stages of cold-air intrusion along the eastern United States, allowing for the coldest air of the different lake-effect types to be positioned in the Lake Champlain Valley (Fig. 6f).

Significant temperature variations were found across the different surface stations during each lake-effect event type (Fig. 7). Temperatures were generally warmest at VMCR, which is positioned over central Lake Champlain (Fig. 1), thereby receiving the most direct modifying influence of surface heat fluxes during lake-effect events. Temperatures were very similar at KBTV and KPLB despite being positioned on different lake shores (eastern vs western) and KPLB having a location farther north by approximately 25 km. A comparison of temperatures at CYHU with those at KBTV and KPLB clearly shows that temperatures at the two nearshore lake stations (KBTV and KPLB) are warmer by upward of 2.5°C on average. These differences are likely a direct result of the proximity of KBTV and KPLB to Lake Champlain and provide a measure of the modifying influence of the lake on atmospheric conditions in the Lake Champlain Valley.

The mean temperatures at KBTV, CYHU, KPLB, and VMCR for LC-North events were −15.9°, −18.1°, −16.3°, and −13.6°C, respectively. Both CYHU and VMCR had temperatures that were significantly different from the other three stations examined. For example, VMCR temperatures were significantly higher than temperatures at CYHU, KPLB, and KBTV. Not surprising is that temperatures at KBTV and KPLB were statistically similar (Fig. 7a) for LC-North events. Similar to what was found for LC-North events, VMCR temperatures for LC-South events were significantly warmer than those of KBTV, KPLB, and CYHU (Fig. 7b). Last, VMCR and CYHU temperatures were significantly different during SYNOP events, though temperatures at either station did not differ significantly from those at KBTV and KPLB (Fig. 7c).

The smaller variation in temperatures overall and between stations during LC-South and SYNOP events shows that these events occur under more restricted conditions and suggests that they are likely more susceptible than LC-North events to slight shifts in the magnitude and frequency of cold-air outbreaks (e.g., Walsh et al. 2001; Portis et al. 2006). Examination of nonevent time periods and interannual climate variations during the nine winters could be utilized to address the impact of slight shifts in seasonal temperature conditions on the frequency of Lake Champlain lake-effect events; however, these analyses are beyond the scope of the current investigation.

Hourly air temperatures measured at VMCR were used with daily water temperatures collected at the KSFD in Burlington to estimate surface $\Delta T$ for each hour during events (Fig. 8). The mean $\Delta T$ for LC-South, LC-North, and SYNOP events was 16.5°, 14.6°, and 12.0°C, respectively. Statistically significant differences were found among the $\Delta T$ for each lake-effect event type. LC-North events exhibited a larger variation in $\Delta T$, with an interquartile range of nearly 6.5°C as compared with an interquartile range of 3.5°C for both LC-South and SYNOP events. As a result of colder temperatures at KBTV, KPLB, and CYHU, $\Delta T$ values estimated using measurements from these stations were greater than those determined from VMCR, where temperatures experienced the largest modification from Lake Champlain. For example, during LC-South events, the coldest on average, mean $\Delta T$ values based on air temperatures at KBTV and KPLB were 22.0° and 21.4°C, respectively. Surface $\Delta T$ values for Lake Champlain lake-effect events were significantly larger than those observed during lake-effect events on the Great Salt Lake. Steenburgh et al. (2000) found mean and maximum $\Delta T$ values of 7.6° and 14.2°C, respectively, for Great Salt Lake lake-effect events that occurred from 1994 to 1998.

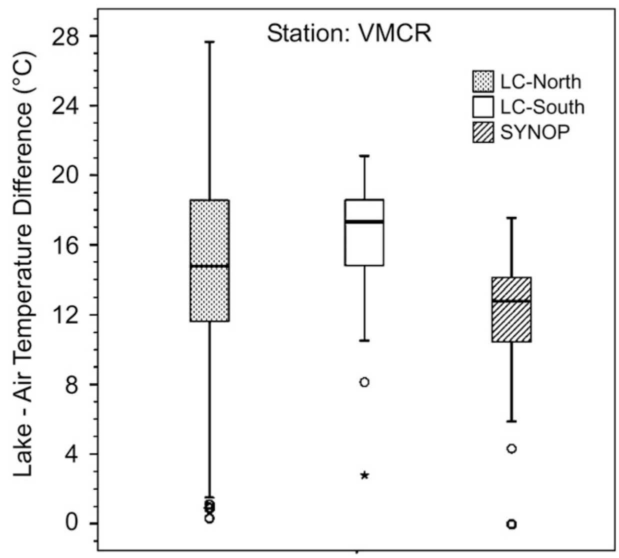


FIG. 8. Box plot of temperature difference between the lake and surface air temperature at VMCR for each lake-effect event type.

### 2) Dewpoint temperature

Dewpoint temperature was used to compare the amount of atmospheric moisture present at the four surface stations during each lake-effect event type (Fig. 9). In general, the positive (lake to atmosphere) latent heat fluxes during lake-effect events greatly increased the atmospheric moisture observed at VMCR relative to conditions at KBTV, KPLB, and CYHU. For LC-North events (Fig. 9a), the dewpoint temperatures at VMCR

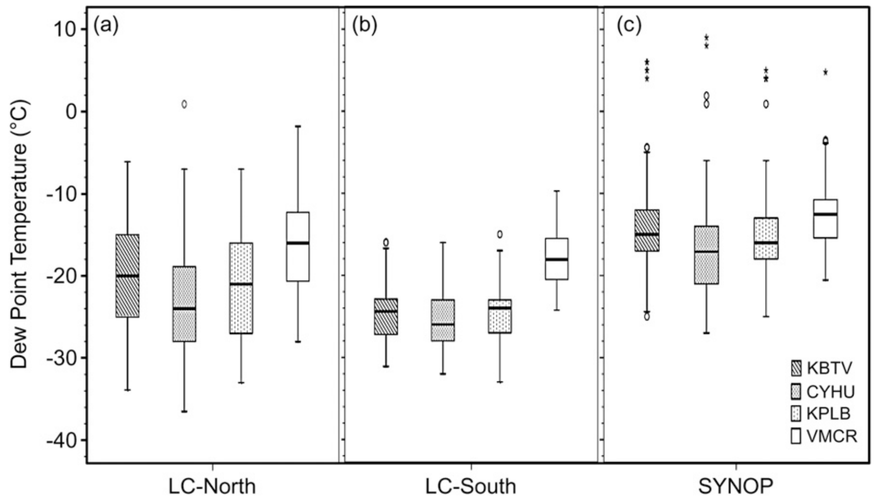


FIG. 9. As in Fig. 7, but for dewpoint temperature (°C).

and CYHU were statistically different (i.e., higher and lower, respectively) from all other stations and dewpoint temperatures at KBTV and KPLB were statistically similar. However, during LC-South events, dewpoint temperatures at CYHU, KBTV, and KPLB were not significantly different (Fig. 9b). It is interesting to note that the moisture content was lower for LC-South events than for LC-North events and the interquartile range was much smaller than existed for LC-North events. Last, SYNOP events were found to have the highest dewpoint temperatures, and measurements at all stations were very similar, with the interquartile ranges extending from −10° to −22°C (Fig. 9c).

### 3) SEA LEVEL PRESSURE

The average SLP was lowest for SYNOP events (1019.6 hPa) and was similar for both LC-North (1025.7 hPa) and LC-South (1024.7 hPa) events. The SLP for SYNOP events is significantly lower when compared with SLP for both LC-North and LC-South events, regardless of station location (Fig. 10). This result is consistent with the large-scale conditions presented in Fig. 6, in which SYNOP events occur in close proximity to an eastward-moving center of low pressure. LC-North events typically develop at a subsequent stage as the large-scale pattern has shifted farther eastward and high pressure moves into the eastern Great Lakes region, and LC-South events occur at the latter stages of the established polar air mass in the presence of a ridge axis.

Regardless of lake-effect event type, the SLP at VMCR is approximately 3–5 hPa lower than the SLP at the other stations (Fig. 10). For example, during LC-North events the average SLP at VMCR, KBTV,

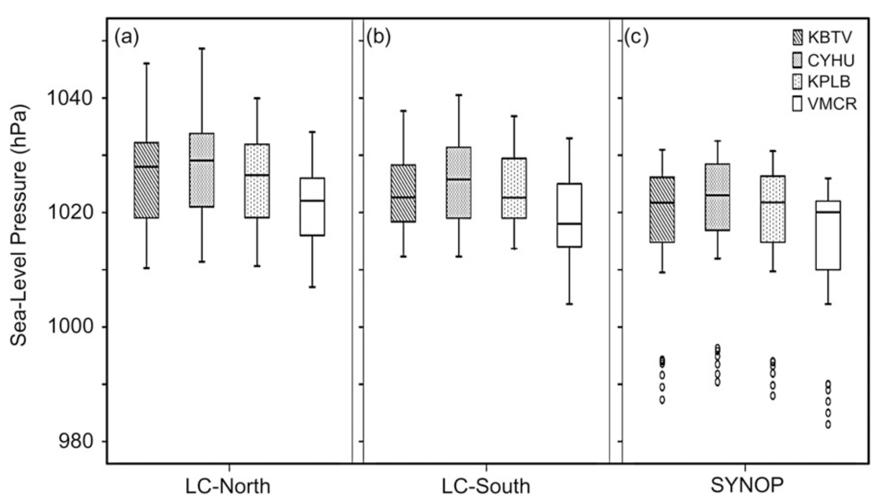


FIG. 10. As in Fig. 7, but for SLP (hPa).

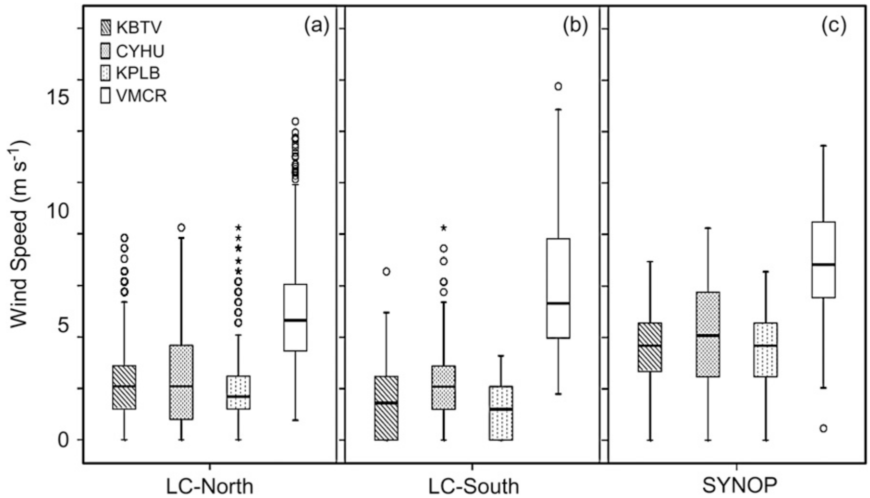


FIG. 11. As in Fig. 7, but for wind speed (m $s^{-1}$).

KPLB, and CYHU was 1021.9, 1026.3, 1024.4, and 1025.9 hPa, respectively. As an example, the maximum difference in SLP between KBTV and VMCR for the 18 January 2003 LC-South event (Fig. 3c) presented by Payer et al. (2007) was 5.3 hPa. These lower VMCR SLP measurements indicate the frequent presence of a mesolow over Lake Champlain as a result of positive heat and moisture fluxes during lake-effect conditions. This feature has not previously been observed for lake-effect storms associated with small lakes, but has frequently been discussed in relation to Great Lakes lake-effect studies (e.g., Braham 1983; Pease et al. 1988; Laird et al. 2003).

#### 4) WIND SPEED AND DIRECTION

On average, SYNOP events had wind speeds that were nearly 60% greater than those of LC-North and LC-South events (Fig. 11). The mean wind speed for SYNOP events was 5.4 m $s^{-1}$, and SYNOP wind speeds were found to be statistically greater than winds observed during LC-North (mean = 3.4 m $s^{-1}$) and LC-South (mean = 3.1 m $s^{-1}$) events. The higher winds during SYNOP events occur in relation to the greater pressure gradient near the western side of an eastward-moving low pressure system (Fig. 6a). The wind speeds decrease for LC-North events, with the associated weakening of the surface pressure gradient as a center of high pressure builds into southern Ontario (Fig. 6c). The lowest wind speeds occur during LC-South events in relation to a weak pressure gradient and the timing of the events immediately following the passage of a northward-extended ridge axis (Fig. 6e).

Wind speeds are consistently the highest over Lake Champlain at VMCR relative to winds measured at the other three surface stations (Fig. 11). For example, average wind speeds for LC-North events at VMCR, KBTV, KPLB, and CYHU were 6.2, 2.9, 2.4, and 2.9 m $s^{-1}$, respectively. The differences in wind speeds across surface stations are statistically significant and consistent regardless of lake-effect event type. The differences indicate that a reduction in surface frictional force over Lake Champlain resulted in wind speeds at VMCR being nearly 2 times the wind speeds at the three other land-based locations.

The frequency of wind speed and direction for each event type is provided in Fig. 12 using measurements from KBTV. Nearly 95% of winds during SYNOP events are from north (55%) or north-northwest (40%) directions. Wind observations during LC-North and LC-South events indicate an important contribution from land breezes, with weak easterly winds at KBTV. The dominant wind direction is along the major axis of Lake Champlain during LC-North and LC-South events, but nearly 40% of either event type had wind directions with a small easterly component between 22.5° and 157.5° (Fig. 12). Wind observations from KPLB during LC-North and LC-South events demonstrated a similar contribution from land breezes along the western shore, with weak westerly winds (not shown).

### d. Soundings and ACARS

A lower-tropospheric stable layer was often present in both the WMW and ALB soundings during lake-effect events. Soundings 1) with a stable layer or inversion at the surface (43 and 17 soundings from WMW and ALB, respectively) or 2) that were characterized by an inversion that was lower than the 925-hPa level but

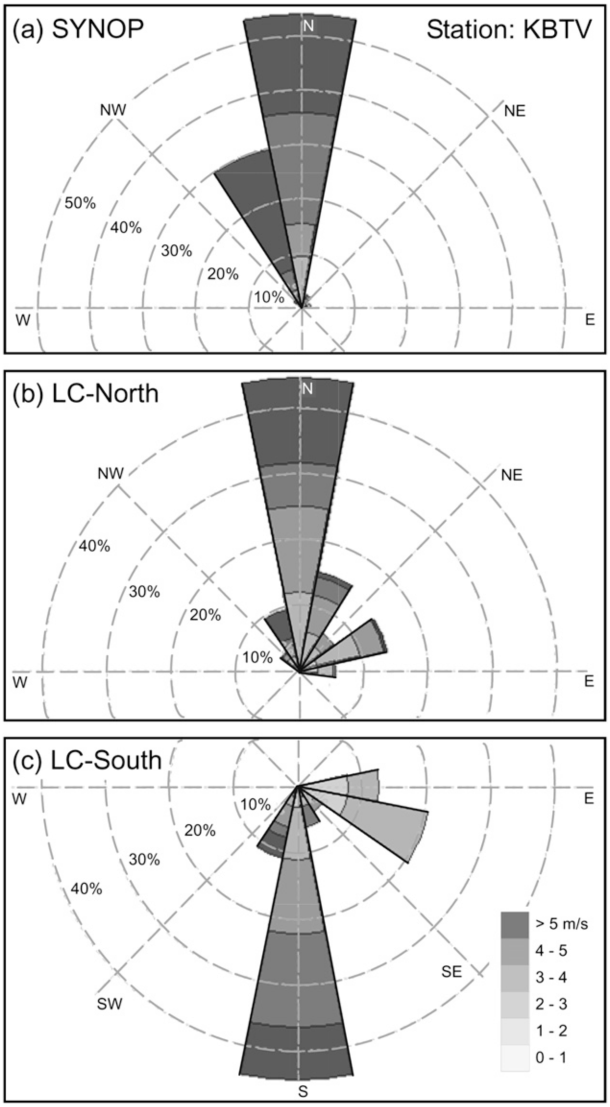


FIG. 12. Wind rose plots showing wind speed and direction information at KBTV during (a) SYNOP, (b) LC-North, and (c) LC-South events.

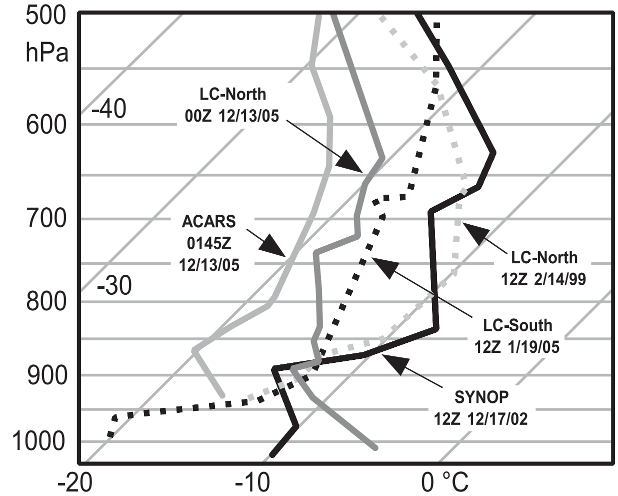


FIG. 13. Representative ALB vertical temperature profiles for each type of Lake Champlain lake-effect event (SYNOP, LC-North, and LC-South) and comparative temperature profiles on 13 Dec 2005 for ACARS and ALB during an LC-North event.

not at the surface (53 soundings) composed 78% of the total 145 soundings. On average, the base of a stable layer that did not reach the surface was positioned at 844, 934, and 948 hPa for SYNOP, LC-North, and LC-South events, respectively. Representative vertical temperature profiles from SYNOP, LC-North, and LC-South events are presented in Fig. 13. The LC-South profile demonstrates that the base of an inversion was generally lower than during the other types of events and that the lower-tropospheric temperatures were often considerably colder, similar to the surface temperature analysis presented in Fig. 7. In general, these variations are consistent with the timing of the events following an eastward-exiting center of low pressure and the stage at which each event type occurs relative to the evolution of the subsequent polar air mass. For example, LC-South events with the lowest stable layer bases occur near the latter stages of the polar air mass as warm advection to the west of the Lake Champlain region begins in association with the approaching warm front and low pressure over the western Great Lakes (Figs. 6e,f).

ACARS soundings available from KBTV were compared with the WMW and ALB soundings at corresponding times to assess whether a lake-modified boundary layer in the Lake Champlain Valley could be observed. ACARS, WMW, and ALB temperature profiles were found to have similar structure with variations at any particular pressure level of generally <5°C. ACARS observations were seldom available for levels below about 900 m (3000 feet) and therefore rarely provided vertical temperature profile information from within the shallow Lake Champlain lake-effect boundary layer. As an example, vertical temperature profiles for ACARS (0145 UTC) and ALB (0000 UTC) on 13 December 2005 are shown in Fig. 13. Although ACARS measurements were not available below 700 m, the ACARS profile shows a deeper mixed layer in the lower troposphere near Lake Champlain as suggested by a comparison of the height of the ALB and ACARS inversion layers.

Based on results from other lake-effect studies (e.g., Carpenter 1993; Kristovich and Laird 1998; Steenburgh et al. 2000), the low altitude of the stable layer or inversion (often at the surface outside the Lake Champlain

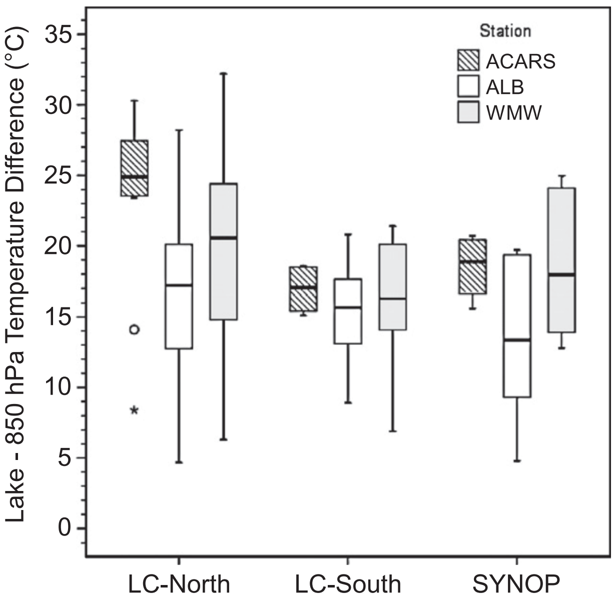


FIG. 14. Box plot showing distribution of temperature difference between lake level and 850-hPa level from soundings at ALB, WMW, and ACARS at KBTV.

Valley) during lake-effect events should tend to significantly limit the development of these events. Although the ACARS soundings do not provide an indication of the thermodynamic profile in the lower troposphere, the significantly higher surface temperatures and dewpoint temperatures observed at VMCR during lake-effect events and the large $\Delta T$ values suggest that Lake Champlain appreciably modified the polar air mass within the valley. The evolution of this modified environment was likely aided by the isolating nature of the orography of the Lake Champlain Valley with the high peaks of the Adirondack Mountains to the west and Green Mountains to the east (Fig. 1).

The temperature difference $\Delta T_{850}$ between the lake surface and 850 hPa was determined using soundings from ACARS, WMW, and ALB (Fig. 14). The mean $\Delta T_{850}$ was 18.2°C, with a minimum of 4.7°C and a maximum of 32.2°C. Differences among lake-effect event types were not statistically significant; however, LC-North events had a larger mean $\Delta T_{850}$ (18.7°C) relative to values for LC-South and SYNOP events (16.0° and 16.6°C, respectively). These values are much larger than criteria suggested as necessary or optimal for a lake-effect environment. Rothrock (1969) and Niziol (1987) found that a lapse rate approximately equivalent to the dry adiabatic lapse rate from the surface to 850 hPa ($\Delta T_{850}$ = 13°C) is typically present during Great Lakes lake-effect storms. Steenburgh et al. (2000) found a similar result for Great Salt Lake lake-effect events in which temperature differences between the lake and 700 hPa exceeded 16°C (i.e., dry adiabatic lapse rate). Nearly 80% of Lake Champlain event $\Delta T_{850}$ values exceeded 13°C, suggesting that during most time periods atmospheric instability existed within the Lake Champlain Valley, although it was not directly observed by ACARS soundings.

## 4. Discussion and summary

The climatological study of Lake Champlain lake-effect precipitation bands provides several unique findings that are useful for comparison with known lake-effect environments for larger lakes (e.g., Great Lakes and Great Salt Lake).

1) There is development of lake-effect precipitation bands over Lake Champlain during southerly wind time periods (i.e., LC-South events). Payer et al. (2007) provided a description of the snowband event that occurred on 18 January 2003 (Fig. 2c); however, the results presented in this article place the 18 January 2003 event in a climatological context, showing that nearly 25% of isolated Lake Champlain lake-effect precipitation bands occur under conditions of southerly winds. To the knowledge of the authors, events of this type have not been reported for any other meridionally oriented lakes (e.g., Lake Michigan or Great Salt Lake).
2) Lake Champlain lake-effect events typically occur with a large difference between lake water temperature and surface air temperature. The average $\Delta T$ for all hourly VMCR observations during event time periods was 14.4°C, with nearly 86% of the $\Delta T$ values >10°C. This is significantly stronger surface forcing than Carpenter (1993) and Steenburgh et al. (2000) found for Great Salt Lake lake-effect events, for which the respective mean $\Delta T$ values were 2.9° and 7.6°C.
3) A lower-tropospheric (<925-hPa level) stable layer or surface inversion was typically present in soundings from ALB and WMW during Lake Champlain events. A near-surface stable layer or surface inversion is often identified as limiting to lake-effect band development. For example, Niziol et al. (1995) list the height and intensity of a subsidence inversion as key forecast variables in assessing the potential for Great Lakes lake-effect snow. Steenburgh et al. (2000) identifies the absence of a capping inversion or stable layer within 150 hPa of the surface as important to lake-effect snow development for the Great Salt Lake. The ability of Lake Champlain lake-effect precipitation to develop within this stable environment suggests that the strong surface forcing

(item 2 above) and presence of the Adirondack Mountains to the west and Green Mountains to the east are significant parameters providing a favorable environmental setting. Further investigation using mesoscale model simulations would be necessary to examine these parameters, especially the influence of topographic forcing on the development and evolution of these shallow, small-lake lake-effect circulations.

4) A large percent (approximately 80%) of $\Delta T_{850}$ values for Lake Champlain events were greater than 13°C, which has been identified as an important criterion for the development of Great Lakes lake-effect snow. In fact, a noteworthy percentage of $\Delta T_{850}$ values (50%) were larger than 18°C, which suggests that the overlake environment was favorable for the development of a well-mixed convective boundary layer and lake-effect snowbands. Previous studies have shown the influence of the Great Lakes on the development of overlake boundary layers (e.g., Young et al. 2000); however, vertical atmospheric profile measurements have not been collected over lakes similar to or smaller in size than Lake Champlain to quantify the impact of the lake on the lower-tropospheric stability during lake-effect events.

It is noteworthy that nearly all Lake Champlain lake-effect precipitation bands developed during cold conditions (i.e., nearshore surface temperatures below 0°C) and that only a single lake-effect event identified during the nine-winter study period had surface temperatures that were above 0°C. The observations suggest that strong surface forcing (i.e., lake surface heat fluxes) is necessary during Lake Champlain events to overcome the limiting lower-tropospheric stability and to create a convective boundary layer capable of initiating shallow mesoscale circulations (e.g., land breeze) and lake-effect snowbands. A natural area for future investigation is an examination of conditions for non-lake-effect precipitation time periods during October–March and the completion of a comparative analysis with the lake-effect climatological description presented in this study.

Although the strong surface forcing allowed for the initiation of lake-effect snowbands, the strength and height of the stable layer (or inversion) had an important role in limiting the vertical development of the lake-effect circulations. ACARS soundings combined with WSR-88D echo heights suggest that Lake Champlain snowbands are often very shallow (i.e., $\leq$1.0 km) relative to the 2–3-km height of Great Lakes lake-effect snowbands (e.g., Braham 1983). The degree of modification to the polar air mass by Lake Champlain and characteristics of the lake-effect boundary layer are certainly linked to the lakewide total energy transfer (e.g., Cordeira and Laird 2008) and spatial scale of Lake Champlain, especially when ice cover is present over areas of the lake. Laird et al. (2003) conducted a series of idealized model simulations examining the influence of lake surface area on lake-effect circulations; however, mesoscale model simulations of several Lake Champlain lake-effect cases, similar to the study performed by Onton and Steenburgh (2001) for the Great Salt Lake, could further address the influence of several factors important to lake-effect snows associated with small lakes.

Previous investigations of lake-effect precipitation events associated with larger lakes (e.g., Niziol et al. 1995; Miner and Fritsch 1997; Laird and Kristovich 2004) have shown the large variability of environmental conditions during lake-effect events. The results of the current investigation show that Lake Champlain lake-effect events occur within a limited range of wind and temperature conditions. These restrictive environmental parameters suggest that small-lake lake-effect events—and, to be specific, Lake Champlain events—may be more sensitive to small changes in environmental conditions than are large-lake lake-effect events and can offer a more responsive system for subsequent investigation of connections between mesoscale processes and climate variability.

*Acknowledgments.* The second and third authors contributed to this research during the 2006 and 2007 summer undergraduate research program at Hobart & William Smith (HWS) Colleges. We are grateful for the support of two additional students in the 2006 research program, Ryan Sobash and Natasha Hodas. The NWS Forecast Office in Burlington, VT, provided access to archived lake water temperature and shared very helpful suggestions and comments during the presentation of our initial findings at their 2006 Winter Weather Workshop. This research was supported by the Office of the Provost at HWS and the National Science Foundation under Grant ATM-0512233. Any opinions, findings, conclusions, and recommendations expressed in this publication are those of the authors and do not necessarily reflect the views of the National Science Foundation.

# APPENDIX

## Lake Champlain Lake-Effect Events

Table A1 lists the timing and type characteristics of the 67 lake-effect events that were identified and examined in this study.

TABLE A1. Characteristics of the 67 Lake Champlain lake-effect events that were examined in this study. Blank rows separate individual winter seasons.

| | Start date | Start time (UTC) | End date | End time (UTC) | Duration (h) | Type |
|---|---|---|---|---|---|---|
| 1 | 21 Dec 1997 | 0657 | 21 Dec 1997 | 1716 | 10.32 | LC-North |
| 2 | 28 Dec 1997 | 0914 | 28 Dec 1997 | 1803 | 8.82 | LC-North |
| 3 | 1 Jan 1998 | 0742 | 1 Jan 1998 | 1840 | 10.97 | LC-South |
| 4 | 17 Jan 1998 | 1009 | 17 Jan 1998 | 1850 | 8.68 | LC-North |
| 5 | 22 Jan 1998 | 0421 | 22 Jan 1998 | 1706 | 12.75 | LC-North |
| 6 | 23 Jan 1998 | 0018 | 23 Jan 1998 | 1055 | 10.62 | LC-Calm |
| 7 | 27 Jan 1998 | 1350 | 27 Jan 1998 | 1631 | 2.68 | LC-North |
| 8 | 14 Feb 1998 | 0123 | 14 Feb 1998 | 1537 | 14.23 | LC-North |
| 9 | 15 Feb 1998 | 0422 | 15 Feb 1998 | 1411 | 9.82 | LC-North |
| | | | | | | |
| 10 | 31 Dec 1998 | 0430 | 1 Jan 1999 | 0438 | 24.13 | LC-Calm |
| 11 | 2 Jan 1999 | 1158 | 2 Jan 1999 | 1750 | 5.87 | LC-South |
| 12 | 13 Jan 1999 | 1227 | 14 Jan 1999 | 1945 | 31.30 | Transitional |
| 13 | 29 Jan 1999 | 0728 | 29 Jan 1999 | 1252 | 5.40 | Transitional |
| 14 | 14 Feb 1999 | 1056 | 14 Feb 1999 | 1520 | 4.40 | LC-North |
| 15 | 22 Feb 1999 | 0740 | 22 Feb 1999 | 1551 | 8.18 | LC-North |
| 16 | 8 Mar 1999 | 0240 | 8 Mar 1999 | 0627 | 3.78 | LC-North |
| | | | | | | |
| 17 | 30 Nov 1999 | 2145 | 1 Dec 1999 | 1609 | 18.40 | LC-North |
| 18 | 15 Jan 2000 | 0334 | 15 Jan 2000 | 1525 | 11.85 | LC-North |
| 19 | 17 Jan 2000 | 1100 | 18 Jan 2000 | 1709 | 30.15 | LC-North |
| 20 | 18 Jan 2000 | 2324 | 19 Jan 2000 | 1749 | 18.42 | LC-North |
| 21 | 23 Jan 2000 | 0753 | 23 Jan 2000 | 1637 | 8.73 | LC-South |
| 22 | 29 Jan 2000 | 0955 | 29 Jan 2000 | 1525 | 5.50 | LC-South |
| 23 | 3 Feb 2000 | 0819 | 3 Feb 2000 | 1544 | 7.42 | LC-South |
| | | | | | | |
| 24 | 8 Dec 2000 | 0536 | 9 Dec 2000 | 1449 | 33.22 | LC-North |
| 25 | 12 Jan 2001 | 1151 | 12 Jan 2001 | 1629 | 4.63 | LC-North |
| 26 | 20 Jan 2001 | 1253 | 20 Jan 2001 | 1810 | 5.28 | LC-North |
| 27 | 21 Jan 2001 | 0124 | 21 Jan 2001 | 1106 | 9.70 | LC-North |
| 28 | 28 Feb 2001 | 0503 | 28 Feb 2001 | 1108 | 6.08 | SYNOP |
| 29 | 22 Dec 2001 | 1034 | 22 Dec 2001 | 1517 | 4.72 | SYNOP |
| 30 | 9 Feb 2002 | 0619 | 9 Feb 2002 | 1313 | 6.90 | LC-North |
| | | | | | | |
| 31 | 27 Nov 2002 | 0606 | 27 Nov 2002 | 1609 | 10.05 | SYNOP |
| 32 | 17 Dec 2002 | 1034 | 17 Dec 2002 | 1637 | 6.05 | Transitional |
| 33 | 30 Dec 2002 | 0917 | 30 Dec 2002 | 1530 | 6.22 | LC-North |
| 34 | 2 Jan 2003 | 0649 | 2 Jan 2003 | 1720 | 10.52 | LC-North |
| 35 | 5 Jan 2003 | 0149 | 5 Jan 2003 | 1509 | 13.33 | Transitional |
| 36 | 9 Jan 2003 | 1140 | 9 Jan 2003 | 1714 | 5.57 | SYNOP |
| 37 | 15 Jan 2003 | 0551 | 16 Jan 2003 | 0136 | 19.75 | Transitional |
| 38 | 17 Jan 2003 | 1330 | 18 Jan 2003 | 0200 | 12.50 | Transitional |
| 39 | 18 Jan 2003 | 0757 | 18 Jan 2003 | 1749 | 9.87 | LC-South |
| 40 | 23 Jan 2003 | 1805 | 24 Jan 2003 | 0221 | 8.27 | SYNOP |
| 41 | 28 Jan 2003 | 0655 | 28 Jan 2003 | 1558 | 9.05 | LC-South |
| | | | | | | |
| 42 | 4 Nov 2003 | 0525 | 4 Nov 2003 | 0635 | 1.17 | SYNOP |
| 43 | 5 Dec 2003 | 0353 | 5 Dec 2003 | 1817 | 14.40 | LC-North |
| 44 | 6 Dec 2003 | 0456 | 6 Dec 2003 | 1200 | 7.07 | LC-North |
| 45 | 21 Dec 2003 | 0440 | 21 Dec 2003 | 0758 | 3.30 | LC-South |
| 46 | 8 Jan 2004 | 2046 | 10 Jan 2004 | 1814 | 45.47 | LC-North |
| 47 | 11 Jan 2004 | 0457 | 11 Jan 2004 | 1450 | 9.88 | Transitional |
| 48 | 14 Jan 2004 | 2024 | 15 Jan 2004 | 1828 | 22.07 | LC-North |
| 49 | 17 Jan 2004 | 0859 | 17 Jan 2004 | 1609 | 7.17 | LC-Calm |

TABLE A1. (*Continued*)

| | Start date | Start time (UTC) | End date | End time (UTC) | Duration (h) | Type |
|---|---|---|---|---|---|---|
| 50 | 10 Nov 2004 | 0509 | 10 Nov 2004 | 0944 | 4.58 | LC-Calm |
| 51 | 15 Dec 2004 | 0251 | 15 Dec 2004 | 1719 | 14.47 | LC-North |
| 52 | 18 Dec 2004 | 0646 | 18 Dec 2004 | 0930 | 2.73 | LC-Calm |
| 53 | 26 Dec 2004 | 0447 | 27 Dec 2004 | 1759 | 37.20 | Transitional |
| 54 | 5 Jan 2005 | 1508 | 6 Jan 2005 | 0448 | 13.67 | Transitional |
| 55 | 17 Jan 2005 | 0455 | 17 Jan 2005 | 1744 | 12.82 | SYNOP |
| 56 | 19 Jan 2005 | 0006 | 19 Jan 2005 | 1437 | 14.52 | LC-South |
| 57 | 23 Jan 2005 | 0742 | 23 Jan 2005 | 2033 | 12.85 | LC-North |
| 58 | 24 Jan 2005 | 1035 | 24 Jan 2005 | 1628 | 5.88 | LC-South |
| 59 | 26 Jan 2005 | 0648 | 26 Jan 2005 | 1929 | 12.68 | SYNOP |
| 60 | 27 Jan 2005 | 0749 | 27 Jan 2005 | 1743 | 9.90 | LC-North |
| 61 | 8 Oct 2005 | 1227 | 8 Oct 2005 | 1659 | 4.53 | SYNOP |
| 62 | 12 Dec 2005 | 2257 | 13 Dec 2005 | 1742 | 18.75 | LC-North |
| 63 | 13 Dec 2005 | 2247 | 15 Dec 2005 | 1620 | 41.55 | LC-North |
| 64 | 21 Dec 2005 | 0949 | 21 Dec 2005 | 1612 | 6.38 | LC-South |
| 65 | 31 Dec 2005 | 0649 | 31 Dec 2005 | 2109 | 14.33 | LC-North |
| 66 | 26 Feb 2006 | 0134 | 26 Feb 2006 | 1156 | 10.37 | SYNOP |
| 67 | 3 Mar 2006 | 0225 | 3 Mar 2006 | 0755 | 5.50 | LC-North |

## REFERENCES


Benson, B., and J. Magnuson, 2006: Global lake and river ice phenology database. National Snow and Ice Data Center/World Data Center for Glaciology, Boulder, CO. [Available online at http://nsidc.org/data/lake_river_ice/.]

Braham, R. R., Jr., 1983: The Midwest snowstorm of 8-11 December 1977. *Mon. Wea. Rev.,* **111,** 253–272.

——, and M. J. Dungey, 1984: Quantitative estimates of the effect of Lake Michigan on snowfall. *J. Climate Appl. Meteor.,* **23,** 940–949.

Burnett, A. W., M. E. Kirby, H. T. Mullins, and W. P. Patterson, 2003: Increasing Great Lake–effect snowfall during the twentieth century: A regional response to global warming? *J. Climate,* **16,** 3535–3542.

Cairns, M. M., R. Collins, T. Cylke, M. Deutschendorf, and D. Mercer, 2001: A lake effect snowfall in Western Nevada - Part I: Synoptic setting and observations. Preprints, *18th Conf. on Weather Analysis and Forecasting/14th Conf. on Numerical Weather Prediction*, Fort Lauderdale, FL, Amer. Meteor. Soc., 329–332.

Carpenter, D. M., 1993: The lake effect of the Great Salt Lake: Overview and forecast problems. *Wea. Forecasting,* **8,** 181–193.

Cordeira, J. M., and N. F. Laird, 2008: The influence of ice cover on two lake-effect snow events over Lake Erie. *Mon. Wea. Rev.,* **136,** 2747–2763.

Cosgrove, B. A., S. J. Colucci, R. J. Ballentine, and J. S. Waldstreicher, 1996: Lake effect snow in the Finger Lakes region. Preprints, *15th Conf. on Weather Analysis and Forecasting*, Norfolk, VA, Amer. Meteor. Soc., 573–576.

Dewey, K. F., 1975: The prediction of Lake Huron lake-effect snowfall systems. *J. Appl. Meteor.,* **14,** 3–7.

Dole, R. M., 1928: Snow squalls of the Lake Region. *Mon. Wea. Rev.,* **56,** 512–513.

Forbes, G. S., and J. H. Merritt, 1984: Mesoscale vortices over the Great Lakes in wintertime. *Mon. Wea. Rev.,* **112,** 377–382.

Gerbush, M. R., D. A. R. Kristovich, and N. F. Laird, 2008: Mesoscale boundary layer and heat flux variations over pack ice–covered Lake Erie. *J. Appl. Meteor. Climatol.,* **47,** 668–682.

Grim, J. A., N. F. Laird, and D. A. R. Kristovich, 2004: Mesoscale vortices embedded within a lake-effect shoreline band. *Mon. Wea. Rev.,* **132,** 2269–2274.

Jiusto, J., and M. Kaplan, 1972: Snowfall from lake-effect storms. *Mon. Wea. Rev.,* **100,** 62–66.

Kalnay, E., and Coauthors, 1996: The NCEP/NCAR 40-Year Reanalysis Project. *Bull. Amer. Meteor. Soc.,* **77,** 437–471.

Kelly, R. D., 1986: Mesoscale frequencies and seasonal snowfalls for different types of Lake Michigan snow storms. *J. Appl. Meteor.,* **25,** 308–312.

Kristovich, D. A. R., and R. A. Steve III, 1995: A satellite study of cloud-band frequencies over the Great Lakes. *J. Appl. Meteor.,* **34,** 2083–2090.

——, and N. F. Laird, 1998: Observations of widespread lake-effect cloudiness: Influences of lake surface temperature and upwind conditions. *Wea. Forecasting,* **13,** 811–821.

——, and M. L. Spinar, 2005: Diurnal variations in lake-effect precipitation near the western Great Lakes. *J. Hydrometeor.,* **6,** 210–218.

——, N. F. Laird, M. R. Hjelmfelt, R. G. Derickson, and K. A. Cooper, 1999: Transitions in boundary layer meso-g convective structures: An observational case study. *Mon. Wea. Rev.,* **127,** 2895–2909.

Kunkel, K. E., N. E. Westcott, and D. A. R. Kristovich, 2002: Assessment of potential effects of climate change on heavy lake-effect snowstorms near Lake Erie. *J. Great Lakes Res.,* **28,** 521–536.

Laird, N. F., and D. A. R. Kristovich, 2004: Comparison of observations with idealized model results for a method to resolve winter lake-effect mesoscale morphology. *Mon. Wea. Rev.,* **132,** 1093–1103.

——, J. Miller, and D. A. R. Kristovich, 2001: Synthetic dual-Doppler analysis of a winter mesoscale vortex. *Mon. Wea. Rev.,* **129,** 312–331.

——, D. A. R. Kristovich, and J. E. Walsh, 2003: Idealized model simulations examining the mesoscale structure of winter lake-effect circulations. *Mon. Wea. Rev.,* **131,** 206–221.

——, R. Sobash, and N. Hodas, 2009: The frequency and characteristics of lake-effect precipitation events associated with the New York State Finger Lakes. *J. Appl. Meteor. Climatol.,* in press.

Manley, T. O., K. Hunkins, J. Saylor, G. Miller, and P. Manley, 1999: Aspects of summertime and wintertime hydrodynamics of Lake Champlain. *Water Resources Monograph, Geophys. Monogr.*, Vol. 14, Amer. Geophys. Union, 67–115.

Miner, T. J., and J. M. Fritsch, 1997: Lake-effect rain events. *Mon. Wea. Rev.,* **125,** 3231–3248.

Niziol, T. A., 1987: Operational forecasting of lake effect snowfall in western and central New York. *Wea. Forecasting,* **2,** 310–321.

——, W. R. Snyder, and J. S. Waldstreicher, 1995: Winter weather forecasting throughout the eastern United States. Part IV: Lake effect snow. *Wea. Forecasting,* **10,** 61–77.

Norton, D. C., and S. J. Bolsenga, 1993: Spatiotemporal trends in lake effect and continental snowfall in the Laurentian Great Lakes, 1951–1980. *J. Climate,* **6,** 1943–1956.

Onton, D. J., and W. J. Steenburgh, 2001: Diagnostic and sensitivity studies of the 7 December 1998 Great Salt Lake–effect snowstorm. *Mon. Wea. Rev.,* **129,** 1318–1338.

Payer, M., J. Desrochers, and N. F. Laird, 2007: A lake-effect snow band over Lake Champlain. *Mon. Wea. Rev.,* **135,** 3895–3900.

Peace, R. L., and R. B. Sykes, 1966: Mesoscale study of a lake effect snow storm. *Mon. Wea. Rev.,* **94,** 495–507.

Pease, S. R., W. A. Lyons, C. S. Keen, and M. R. Hjelmfelt, 1988: Mesoscale spiral vortex embedded within a Lake Michigan snow squall band: High resolution satellite observations and numerical model simulations. *Mon. Wea. Rev.,* **116,** 1374–1380.

Portis, D. H., M. P. Cellitti, W. L. Chapman, and J. E. Walsh, 2006: Low-frequency variability and evolution of North American cold air outbreaks. *Mon. Wea. Rev.,* **134,** 579–597.

Remick, J. T., 1942: The effect of Lake Erie on the local distribution of precipitation in winter (I). *Bull. Amer. Meteor. Soc.,* **23,** 111–117.

Rodriguez, Y., D. A. R. Kristovich, and M. R. Hjelmfelt, 2007: Lake-to-lake cloud bands: Frequencies and locations. *Mon. Wea. Rev.,* **135,** 4202–4213.

Rothrock, H. J., 1969: An aid in forecasting significant lake snows. Tech. Memo. WBTM CR-30, National Weather Service Central Region, 16 pp.

Schultz, D. M., 1999: Lake-effect snowstorms in northern Utah and western New York with and without lightning. *Wea. Forecasting,* **14,** 1023–1031.

——, D. S. Arndt, D. J. Stensrud, and J. W. Hanna, 2004: Snowbands during the cold-air outbreak of 23 January 2003. *Mon. Wea. Rev.,* **132,** 827–842.

Sobash, R., H. Carr, and N. F. Laird, 2005: An investigation of New York State Finger Lakes snow band events. Preprints, *11th Conf. on Mesoscale Processes*, Albuquerque, NM, Amer. Meteor. Soc., P3M.3. [Available online at http://ams.confex.com/ams/pdfpapers/96743.pdf.]

Steenburgh, W. J., and D. J. Onton, 2001: Multiscale analysis of the 7 December 1998 Great Salt Lake–effect snowstorm. *Mon. Wea. Rev.,* **129,** 1296–1317.

——, S. F. Halvorson, and D. J. Onton, 2000: Climatology of lake-effect snowstorms of the Great Salt Lake. *Mon. Wea. Rev.,* **128,** 709–727.

Tardy, A., 2000: Lake-effect and lake-enhanced snow in the Champlain Valley of Vermont. Tech. Memo. 2000-05, NWS Eastern Region, 27 pp.

Walsh, J. E., A. S. Phillips, D. H. Portis, and W. L. Chapman, 2001: Extreme cold outbreaks in the United States and Europe, 1948–99. *J. Climate,* **14,** 2642–2658.

Watson, J. S., M. L. Jurewicz, R. J. Ballentine, S. J. Colucci, and J. S. Waldstreicher, 1998: High resolution numerical simulations of Finger Lakes snow bands. Preprints, *16th Conf. on Weather Analysis and Forecasting*, Phoenix, AZ, Amer. Meteor. Soc., 308–310.

Weiss, C. C., and P. J. Sousounis, 1999: A climatology of collective lake disturbances. *Mon. Wea. Rev.,* **127,** 565–574.

Wilken, G. R., 1997: A lake-effect snow in Arkansas. NWS/NOAA Tech. Attachment SR/SSD 97-21, 3 pp.

Young, G. S., B. K. Cameron, and E. E. Hebble, 2000: Observations of the entrainment zone in a rapidly entraining boundary layer. *J. Atmos. Sci.,* **57,** 3145–3160.